

INELASTIC INTERACTIONS OF ^{16}O NUCLEI WITH EMULSION AT 3.7 AGeV

Sabina LEHOČKÁ, Stanislav VOKÁL, Adela KRAVČÁKOVÁ

Institute of Physics, Faculty of Science, P. J. Šafárik University, Jesenná 5, 041 54 Košice, E – mail: sabinka@pobox.sk

SUMMARY

In this work the multiplicities and the angular distributions of secondary charged particles produced in interactions of oxygen nuclei ^{16}O with photoemulsion nuclei at energy 3.7 GeV per nucleon are presented. The dependence of the multiplicities and the angular distributions on the centrality of interaction and also on the energy and on the mass numbers of primary nuclei has been studied. Obtained results have been compared with calculations from cascade – evaporation model.

The average multiplicity of relativistic particles increases rapidly with the mass number of the projectile nucleus A_p . The multiplicity of fast target fragments also increases with the mass number of primary nuclei A_p , while the multiplicity of slow target nucleus fragments is independent on A_p . There are three local maxima observed in the distribution of the multiplicities of target fragments (h – particles) reflecting the size of the target nuclei in photoemulsion the nuclei ^{16}O interacted with. The correlation between the N_h and the summary charge Q of the noninteracting fragments of primary nucleus has been also investigated. The dependence of angular distribution parameters on the centrality of interaction has been analysed. The average values $\langle \cos\theta_i \rangle$ of slow target nucleus fragments (b – particles) and fast target fragments (g – particles) depend very weakly on the centrality degree, but the angular spectra of relativistic particles depends strongly as on desintegration of the nuclei so on the centrality degree too. The used model describes the studied characteristics of secondary particles well. There are some disagreements in the angular distributions of target fragments. This statement can be connected with collective behaviour of nucleus – nucleus interactions.

Keywords: multiplicity, angular distribution, pseudorapidity, nuclear interactions, photoemulsion

1. INTRODUCTION

The present work deals with the study of basic experimental characteristics of secondary charged particles produced in interactions of ^{16}O nuclei with photoemulsion nuclei at energy 3.7 GeV per nucleon. The multiplicity and the angular distributions of secondary particles yield certain information on the production mechanism. The characteristics of secondary charged particles differ from each other according to the energy and the mass of primary nucleus. Our experimental results are compared with the modified cascade – evaporation model (CEM) [6].

2. EXPERIMENTAL PROCEDURE

The presented data were obtained with conventional emulsion stacks. The photoemulsion detector was irradiated horizontally in the Laboratory of High Energies JINR at Dubna by oxygen beam with an energy of 3.7 GeV per nucleon. For the analysis 2823 events of interactions ^{16}O +emulsion measured along the tracks of primary nuclei were used within the EMU01 collaboration [7]. For all charged particles the polar θ and azimuthal Ψ emission angles were determined. The charged secondary particles were divided into the following types in accordance with ordinary photoemulsion methodical criteria:

s – particles (shower): Singly charged relativistic particles with a velocity $\beta \geq 0.7$. These are predominantly pions and protons produced over the whole region of phase space.

h – particles (heavily ionizing particles): Target fragments which include *g* – particles (grey) – fast target fragments with a range in emulsion ≥ 3 mm and having a velocity $\beta < 0.7$; and *b* – particles (black) – charged particles with the range < 3 mm, slow target fragments mainly evaporation products from the remnant of the target nucleus.

3. EXPERIMENTAL RESULTS

3.1. Multiplicity of secondary particles

Tab. 1 shows the average multiplicity values of different secondary particles in collisions of ^{16}O nuclei with emulsion at 3.7 GeV per nucleon in comparison with the average multiplicity values of other primary nuclei at the same energy [3, 4].

Tab. 1 The average multiplicity values for different primary nuclei at energy 3.7 GeV per nucleon.

Primary nucleus	$\langle N_s \rangle$	$\langle N_g \rangle$	$\langle N_b \rangle$
^1H	1.6 ± 0.1	2.8 ± 0.1	3.8 ± 0.1
^4He	3.4 ± 0.1	4.6 ± 0.2	4.7 ± 0.2
^{16}O	9.8 ± 0.2	6.1 ± 0.1	4.6 ± 0.1
^{32}S	13.0 ± 0.4	6.2 ± 0.2	3.7 ± 0.1

The mean multiplicity of relativistic particles increases rapidly with increasing projectile mass number A_p . The distribution of the average

multiplicity of relativistic particles on the mass A_p can be approximated with a power function: $\langle N_s \rangle = 1.55A_p^{0.63}$. The multiplicity of g – particles also increases with increasing the mass number of primary nuclei A_p ($\langle N_g \rangle = 3.01A_p^{0.23}$), while the average multiplicity of b – particles is conservative on A_p . The average numbers of slow target fragments are about the same: $\langle N_b \rangle \approx 4$.

In tab. 2 the average multiplicity values of different secondary particles in collisions of ^{16}O nuclei with emulsion at different energies, from 3.7 to 200 GeV per nucleon [1], are indicated. In parentheses for our energy the results of theoretical calculations are given obtained from the cascade – evaporation model.

Tab. 2 The average multiplicity values of secondary particles at different energies of primary nuclei ^{16}O .

Energy (AGeV)	$\langle N_s \rangle$	$\langle N_g \rangle$	$\langle N_b \rangle$
3.7	9.8 ± 0.2 (11.2 ± 0.2)	6.1 ± 0.1 (6.5 ± 0.1)	4.6 ± 0.1 (5.6 ± 0.1)
14.6	20.3 ± 0.8	5.2 ± 0.2	4.8 ± 0.2
60	39.0 ± 2.1	5.7 ± 0.4	4.5 ± 0.2
200	56.5 ± 2.7	4.3 ± 0.3	4.1 ± 0.2

The average multiplicity of relativistic particles increases rapidly with increasing projectile energy E_p , the best fit is: $\langle N_s \rangle = 5.85E_p^{0.44}$. This tendency relates with rising of the flow of relativistic particles, like pions and protons, with the increase of the energy E_p . One can see independence (or small decrease) in the average values for the target fragments, i. e. b – and g – particles, going up in energy scale.

The multiplicity distribution of the target fragments (h – particles) is shown in Fig. 1a together with the corresponding CEM calculation. A qualitatively good description of the experimental data is obtained by using cascad code. In multiplicity distribution of the h – particles we can observe three local maxima. These maxima determinate the size of the target nuclei in photoemulsion, which the primary ^{16}O nucleus interacted with. The first region in the interval $N_h \in \langle 0;1 \rangle$ represents the interactions of primary nucleus with a hydrogen nucleus. The second region with maximum at $N_h = 6$ is composed by the collisions with a light nuclei of photoemulsion: ^{12}C , ^{14}N and ^{16}O . These two regions include also the

peripheral interactions with the heavy target component in emulsion, i. e. silver and bromine. The third region by the upper values of N_h presents the central interactions with ^{80}Br , ^{108}Ag nuclei.

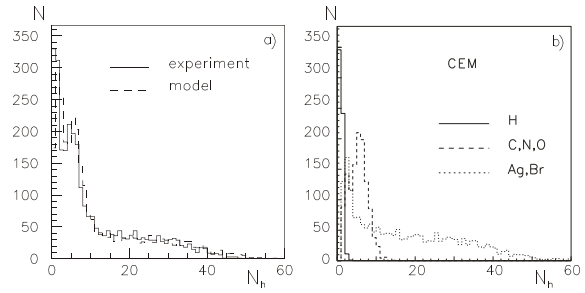


Fig. 1a) The multiplicity distribution of the target fragments compared with the CEM, **b)** The distributions of N_h for different nuclei of photoemulsion predicted by the CEM.

With the cascade – evaporation model we can well distinguish the interactions of oxygen nuclei with different nuclei of photoemulsion, as is shown in the Fig. 1b. Thus, according to the number of target fragments N_h we can determinate the photoemulsion nucleus the ^{16}O interacted with.

3.2. Total charge Q distribution

It is interesting to study the dependence of the multiplicity of charged secondary particles on the charge flow Q of the secondary relativistic fragments, which have not interacted with emulsion nuclei. The total charge of these particles was calculated using the formula $Q = \sum n_i Z_i$, where n_i is the number of fragments having charge Z_i in a given event of interaction.

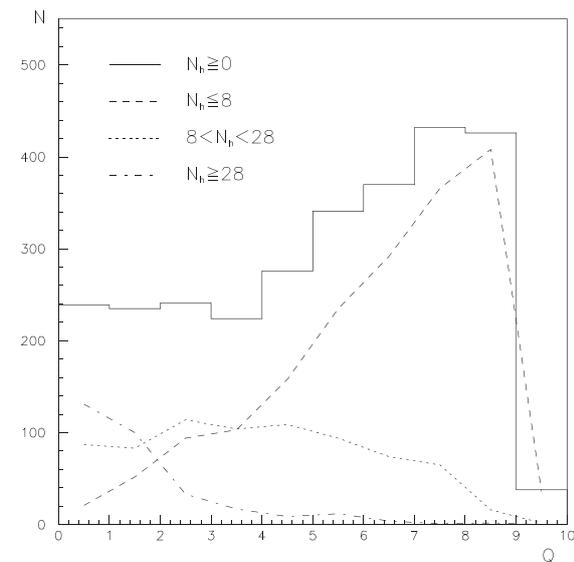


Fig. 2 The experimental distribution of the total charge Q for different groups of N_h .

The value of the total charge Q ranges from zero (every charged nucleon of ^{16}O interacted – central collision) to eight (none of nucleons has been interacted). The value of Q seems to be a conventional experimental value, which can be used for classification of nucleus – nucleus interactions according to the degree of the "centrality" of collisions.

The Q distribution is given in Fig. 2. The quasicentral and peripheral interactions dominate in the present experiment.

The relation between N_h and Q is also shown in Fig. 2. This correlation is presented for three different groups: $N_h \leq 8$, $8 < N_h < 28$ and $N_h \geq 28$. In the first one ($N_h \leq 8$) dominate the largest values of total charge Q . That group represents the collisions of ^{16}O with light nuclei ^1H , ^{12}C , ^{14}N , ^{16}O , but it includes the peripheral interactions with ^{80}Br and ^{108}Ag nuclei too. The second group, where interacted about a half charged nucleons from oxygen nuclei ^{16}O , consists of quasicentral collisions with ^{80}Br and ^{108}Ag nuclei. The third group ($N_h \geq 28$) with the smallest values of Q includes the central interactions with ^{80}Br , ^{108}Ag nuclei.

3.3. Angular distributions

The angular distributions of slow and fast target fragments and relativistic particles are shown in Figs. 3, 4.

The angular spectrum of slow target fragments compared with the theoretical calculations for ^{16}O experiment is presented in Fig. 3a. There is a broad maximum at $\cos\theta_b \sim 0.7$. Similar maxima appear in the angular distributions of slow target fragments in other (^{22}Ne , ^{84}Kr) experiments [2, 5]. These maxima can be interpreted following the conceptions about the collective (hydrodynamic) behaviour of nucleus – nucleus interactions [2]. The angular distribution of slow target fragments (b – particles) is described by a broken line with a break at $\cos\theta_b = 0.1$. At higher energies (from 14.7 to 200 GeV per nucleon) of the primary ^{16}O nucleus the break is at value $\cos\theta_b = -0.5$ [1]. But we don't observe this break in the theoretical distribution given by CEM. The average values of experimental and theoretical distributions are: $\langle \cos\theta_b \rangle_{\text{EXP}} = 0.07 \pm 0.01$ and $\langle \cos\theta_b \rangle_{\text{CEM}} = 0.06 \pm 0.01$.

Fig. 3b presents the angular spectrum of fast target fragments compared with the theoretical calculations according to CEM for ^{16}O experiment. The emission of g – particles dominate at small angles, i. e. the forward emission. The angular distribution of fast target fragments is fitted with exponential function $e^{b \cdot \cos\theta_g}$. The slope parameter b compared with the parameters for ^{16}O nuclei at 200 GeV per nucleon [1] and ^{28}Si nuclei at 3.7 GeV per nucleon [5] is given in tab. 3.

Tab. 3 The fitting parameters b for the angular distribution of fast target fragments.

Primary nucleus	Energy (AGeV)	Parameter b
^{16}O	3.7	1.21
^{16}O	200	0.92
^{28}Si	3.7	1.30

The forward emission of fast target fragments is upper for the larger projectile nucleus at the same energy. With increasing the primary energy of nuclei the rate of forward emitted g – particles decreases.

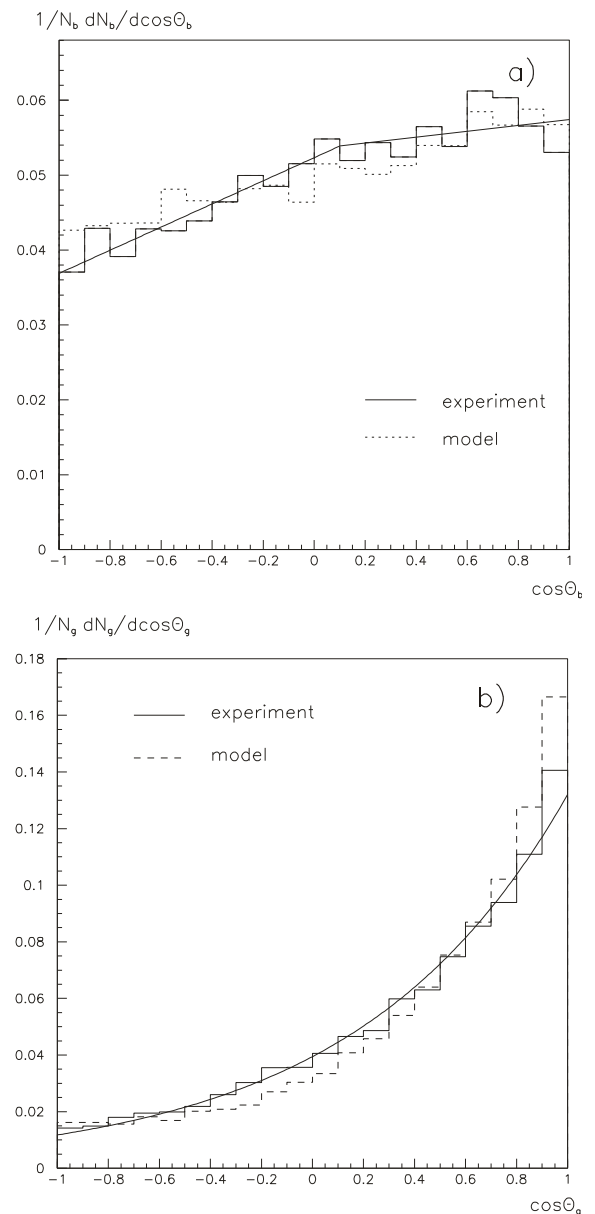


Fig. 3 The angular spectra of a) slow target fragments, b) fast target fragments.

The model describes the angular spectrum of fast fragments relatively good, but in range of small angles overestimates the emission of g – particles. The mean values of experimental and theoretical distributions are: $\langle \cos\theta_g \rangle_{\text{EXP}} = 0.37 \pm 0.01$ and $\langle \cos\theta_g \rangle_{\text{CEM}} = 0.42 \pm 0.01$. The angular spectrum of slow and fast target fragments depends very weakly on the degree of centrality (not presented here).

Fig. 4 presents the pseudorapidity spectrum of relativistic particles given by CEM. With the theoretical calculations we can identify protons, pions and other particles. The ratio between protons and pions predicted by CEM is about the same. It is 1 : 1.17. The cascade – evaporation model describes the experimental data very well. The mean values of the experimental and theoretical distributions are: $\langle \eta_s \rangle_{\text{EXP}} = 2.11 \pm 0.01$ and $\langle \eta_s \rangle_{\text{CEM}} = 2.09 \pm 0.01$. The angular spectrum of relativistic particles depends strongly on centrality degree (not presented here).

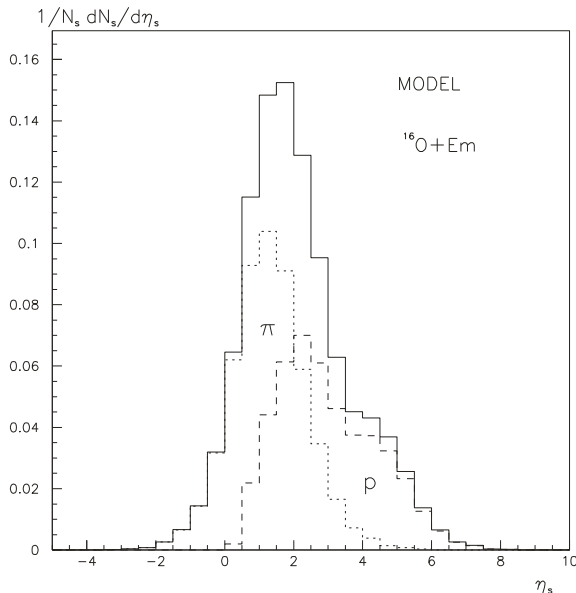


Fig. 4 The angular spectra of relativistic particles given by CEM.

4. CONCLUSION

In present work we have studied the basic characteristics of the inelastic interactions of oxygen nuclei with photoemulsion at energy 3.7 GeV per nucleon. The main results are:

- The average multiplicity of relativistic particles increases rapidly with increasing projectile mass number A_p . The multiplicity of fast target fragments also increases with increasing A_p , while the mean multiplicity of slow target fragments is independent on A_p .
- There are three local maxima observed in the distribution of the multiplicities of target fragments N_h reflecting the size of the target

nuclei in photoemulsion, which the nuclei ^{16}O interacted with.

- The peripheral interactions dominate in the present experiment.
- The average values $\langle \cos\theta_i \rangle$ of slow and fast target fragments depend very weakly on the centrality degree, while the angular spectra of relativistic particles depends strongly on the centrality degree.
- The cascade – evaporation model describes the studied characteristics of secondary particles well. There are some disagreements at the angular distributions of target fragments. This statement can be connected with collective nature of nucleus – nucleus interactions.

REFERENCES

- [1] Adamovich, M. I. et al.: Slow Target Associated Particles Produced in Ultrarelativistic Heavy – Ion Interactions, Preprint LUIP 9103, Lund, 1991
- [2] Andreeva, N. P. et al.: Multiplicities and Angular Distributions of Charged Particles in the Interactions of Neon-22 Nuclei in the Photoemulsion at 4.1 AGeV/c, Preprint OIJA P1–86–8, Dubna, 1986 (in Russian)
- [3] Bannik, B. P. et al.: Inelastic interactions of protons with photoemulsion nuclei at 4.5 GeV/c, Czechoslovak Journal of Physics, B31, pp. 490, 1981
- [4] Kravčáková, A. et al.: Secondary Particles in Nuclear Interactions of ^{32}S in Photoemulsion at Energy 3.7 GeV per nucleon, Proc. of the 13th Conference of Slovak and Czech Physicists, Zvolen, pp. 84, 1999 (in Slovak)
- [5] Kravčáková, A., Vokál, S. : Angular Spectra of Secondary Particles in Interactions of ^{84}Kr in Emulsion at Energy 0.8 – 0.95 GeV per nucleon, Proc. of the 13th Conference of Slovak and Czech Physicists, Zvolen, pp. 81, 1999 (in Slovak)
- [6] Musulmanbekov, G. J. : Modified Cascade Model of Nucleus – Nucleus Collisions, Proc. of the 11th EMU01 Collaboration Meeting, Dubna, pp. 288, 1992
- [7] Vokál, S. et al. (EMU01) : Proc. of the 11th EMU01 Collaboration Meeting, Dubna, pp. 275, 1992

ACKNOWLEDGEMENT

Financial support from the Grant Agency for Science at the Ministry of Education of Slovak Republic and the Slovak Academy of Science (Grant No. 1/9036/02) are cordially acknowledged.